




## FULL PAPER

# New *N*-phenylacetamide-linked 1,2,3-triazole-tethered coumarin conjugates: Synthesis, bioevaluation, and molecular docking study

Satish V. Akolkar<sup>1</sup>  | Amol A. Nagargoje<sup>1,2</sup> | Mubarak H. Shaikh<sup>1,3</sup> |  
Murad Z. A. Warshagha<sup>1</sup> | Jaiprakash N. Sangshetti<sup>4</sup>  | Manoj G. Damale<sup>5</sup> |  
Bapurao B. Shingate<sup>1</sup> 

<sup>1</sup>Department of Chemistry, Dr. Babasaheb Ambedkar Marathwada University, Aurangabad, India

<sup>2</sup>Department of Chemistry, Khopoli Municipal Council College, Khopoli, India

<sup>3</sup>Department of Chemistry, Radhabai Kale Mahila Mahavidyalaya, Ahmednagar, India

<sup>4</sup>Department of Pharmaceutical Chemistry, Y. B. Chavan College of Pharmacy, Dr. Rafiq Zakaria Campus, Aurangabad, India

<sup>5</sup>Department of Pharmaceutical Chemistry, Srinath College of Pharmacy, Aurangabad, India

## Correspondence

Bapurao B. Shingate, Department of Chemistry, Dr. Babasaheb Ambedkar Marathwada University, Aurangabad 431 004, India.  
Email: [bapushingate@gmail.com](mailto:bapushingate@gmail.com)

## Abstract

A series of new 1,2,3-triazole-tethered coumarin conjugates linked by *N*-phenylacetamide was efficiently synthesized via the click chemistry approach in excellent yields. The synthesized conjugates were evaluated for their in vitro antifungal and antioxidant activities. Antifungal activity determination was carried out against fungal strains such as *Candida albicans*, *Fusarium oxysporum*, *Aspergillus flavus*, *Aspergillus niger* and *Cryptococcus neoformans*. Compounds **7b**, **7d**, **7e**, **8b** and **8e** displayed higher potency than the standard drug miconazole, with lower minimum inhibitory concentration values. Also, compound **7a** exhibited potential radical scavenging activity as compared with the standard antioxidant butylated hydroxytoluene. In addition, a molecular docking study of the newly synthesized compounds was carried out, and the results showed a good binding mode at the active site of the fungal (*C. albicans*) P450 cytochrome lanosterol 14 $\alpha$ -demethylase enzyme. Furthermore, the synthesized compounds were also tested for ADME properties, and they demonstrated potential as good candidates for oral drugs.

## KEYWORDS

ADME properties, antifungal activity, antioxidant activity, molecular docking, triazole-coumarin conjugates

## 1 | INTRODUCTION

The incidence of systemic fungal infection has increased dramatically in recent years due to an increase in the number of patients undergoing anticancer chemotherapy and organ transplantation, and AIDS patients.<sup>[1]</sup> Fungi are vital opportunistic human pathogens that have become drug-resistant to many approved compounds, especially *Cryptococcus neoformans*, *Candida*, and *Aspergillus* species, with serious potential consequences. The commonly used azole-based antifungal agents are miconazole, fluconazole, voriconazole, and itraconazole, which showed a wide range of antifungal activity.<sup>[2]</sup> Azoles, especially triazole-based antifungal agents (e.g., voriconazole, fluconazole, and posaconazole) are

widely used for the prevention and treatment of fungal infections (Figure 1). These antifungal drugs inhibit CYP51 (P450 cytochrome lanosterol 14 $\alpha$ -demethylase), a key enzyme in ergosterol biosynthesis.<sup>[3]</sup> However, extensive use of these drugs has resulted in severe drug resistance.<sup>[4]</sup> Therefore, the development of more potent, broad-spectrum antifungal agents with fewer side effects and improved efficiency to cure fungal infections is urgently required.

To counteract the harmful effects of free radicals and other oxidants, the human body has a complex system of natural enzymatic and nonenzymatic antioxidants. Free radicals are unstable chemical species having unpaired electrons that are extremely reactive toward other species. The action of reactive oxygen species (ROS) results in

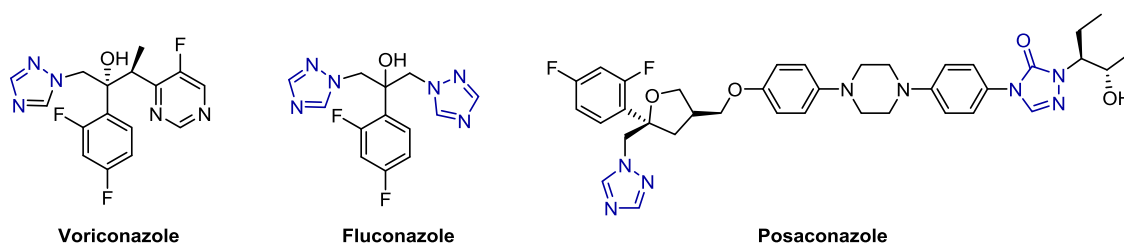


**FIGURE 1** 1,2,4-Triazole-based antifungal drugs

key biomolecules being altered and modulated in function. There is a delicate balance between producing and removing free radicals in healthy organisms. Triazole–coumarin conjugates have unique potential to scavenge ROS such as hydroxyl and superoxide radicals.<sup>[5]</sup> Therefore, the synthesis and development of new antioxidants having the triazole–coumarin pharmacophore have enormous significance in medicinal chemistry.

Diversely functionalized 1,2,3-triazole derivatives have attracted great attention due to their extensive biological properties such as antioxidant,<sup>[5]</sup> antifungal,<sup>[6,7]</sup> antitubercular,<sup>[8]</sup> antibacterial,<sup>[9]</sup> anticancer,<sup>[10]</sup> anti-HIV,<sup>[11]</sup> antimicrobial,<sup>[12]</sup> and antimalarial activity.<sup>[13]</sup> The 1,4-disubstituted-1,2,3-triazoles were synthesized *via* copper-catalyzed azide–alkyne cycloaddition reaction, well known as a click chemistry reaction.<sup>[14]</sup> In the field of medicinal chemistry and drug discovery, 1,2,3-triazoles have received<sup>[15–19]</sup> increasing attention since Sharpless group introduced the “click chemistry” concept. The promising properties of the 1,2,3-triazole ring, such as hydrogen bonding capability, rigidity, stability under *in vivo* conditions, and moderate dipole character, could be helpful for binding of biomolecular targets and increasing solubility.<sup>[15,20,21]</sup> Moreover, 1,2,3-triazoles have become increasingly useful and important in the construction of bioactive and functional molecules as attractive linker units that could connect two pharmacophores to provide innovative bifunctional drugs.<sup>[22–24]</sup> Many drugs available in the market contain 1,2,3-triazole core in their structure, such as cefatrizine (antibiotic), carboxyamidotriazole (anticancer agent), rufinamide (anticonvulsant) and tazobactam (antibacterial agent; Figure 2).

Synthesis of new heterocycles with multiple biological activities remains an interest of the researchers. Among the oxygen heterocycles, coumarins are the privileged structural motifs commonly found in many natural products. Literature reveals that coumarin and its derivatives are isolated from plant-associated endophytes and

display potential biological activities.<sup>[25–29]</sup> In recent years, coumarin-based hybrid molecules have attracted intense interest due to their diverse biological properties.<sup>[30,31]</sup> Different nitrogen-containing heterocycles (e.g., triazole, thiazolidine, thiazole, etc.) in conjunction with coumarin backbone significantly increase the antimicrobial efficiency and also broaden antimicrobial spectrum of these compounds.<sup>[32–34]</sup>

Due to the rapid and effective distribution of privileged systems with relatively improved biological properties as compared with individual entities, the molecular hybridization approach has established eminence over the past few years.<sup>[35]</sup> With strong drug-like properties and desirable binding interactions, these hybrid molecules have emerged for further chemical modifications as structurally novel chemotypes with several exploitable sites. In recent years, a library of coumarin–triazole conjugates was synthesized and proved to enhance biological activity.<sup>[36–39]</sup> There are various reports on the synthesis of coumarin–triazole conjugates with antifungal activity.<sup>[32,38,40,41]</sup> Therefore, the design and synthesis of coumarin–triazole conjugates is crucial for the enhancement of activity.

In continuation of our previous works<sup>[40,42–51]</sup> on the synthesis and biological evaluation of heterocycles, and the significance of coumarin and 1,2,3-triazole moieties in a single molecular framework, herein, we would like to report the design and syntheses of new *N*-phenylacetamide-linked coumarin–triazole conjugates by using the molecular hybridization approach (Figure 3).

The 1,2,3-triazole moiety is good for antifungal activity, and coumarin derivatives have been well reported for the antioxidant activity. Thus, we have evaluated the synthesized compounds for their antifungal and antioxidant activities. The computational parameters like docking study for antifungal activity and ADME (absorption, distribution, metabolism, and elimination) prediction of synthesized coumarin–triazole conjugates were also performed.

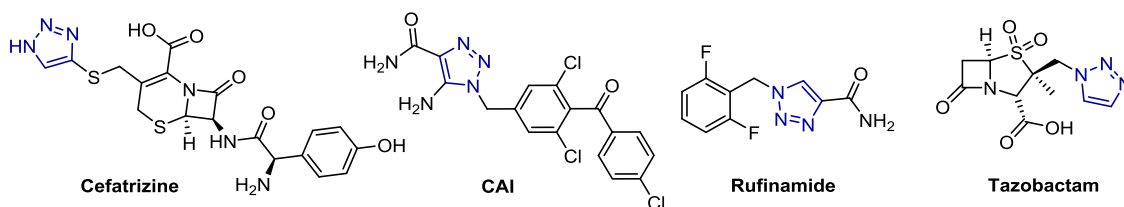


**FIGURE 2** Marketed drugs containing the 1,2,3-triazole unit

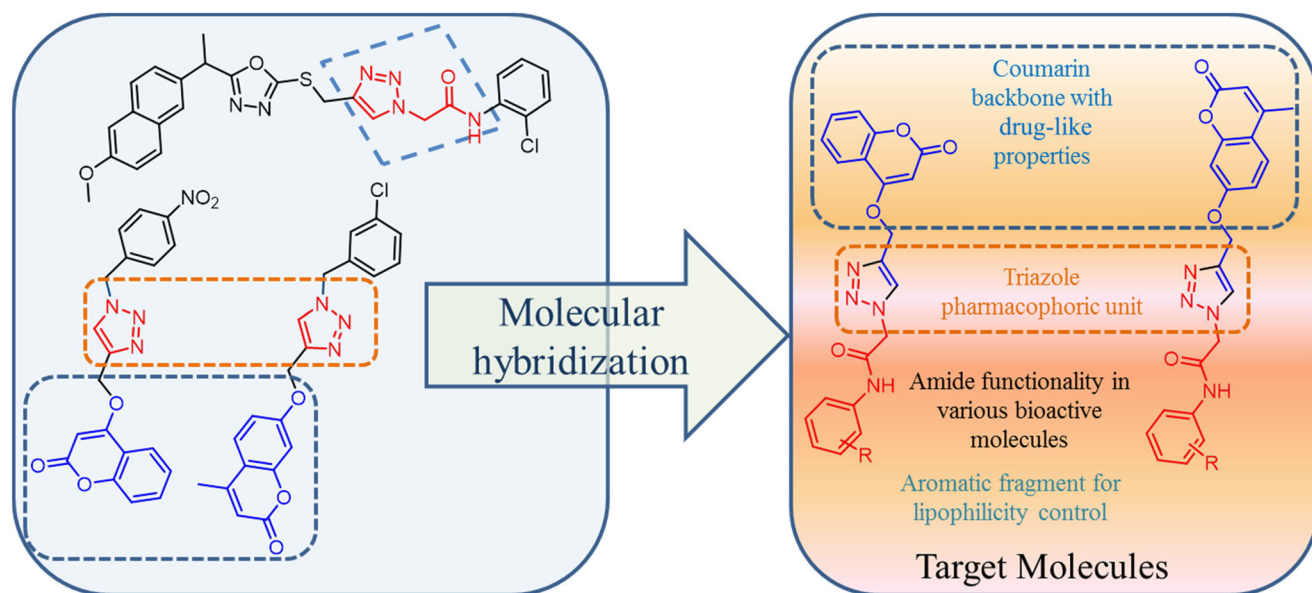


**FIGURE 3** The design strategy for the synthesis of new *N*-phenylacetamide-linked 1,2,3-triazole-coumarin conjugates

## 2 | RESULTS AND DISCUSSION

### 2.1 | Chemistry

1,4-Disubstituted-1,2,3-triazoles bearing amide functionality displayed several biological activities.<sup>[52–55]</sup> On the basis of these reports and molecular hybridization concept, we have designed and synthesized coumarin–triazole conjugates with amide linkage in their structures. A library of substituted 2-(4-[[[4-methyl-2-oxo-2*H*-chromen-7-yl]oxy]methyl]-1*H*-1,2,3-triazol-1-yl)-*N*-phenylacetamides **7a–g** and substituted 2-(4-[[[2-oxo-2*H*-chromen-4-yl]oxy]methyl]-1*H*-1,2,3-triazol-1-yl)-*N*-phenylacetamides **8a–g** was synthesized from commercially available starting materials. These compounds were constructed by the fusion of coumarin-based alkynes and substituted 2-azido-*N*-phenylacetamides *via* the click chemistry approach (Scheme 1).

The starting materials, 2-azido-*N*-phenylacetamides **3a–g**, were prepared by a previously reported method<sup>[45,51]</sup> from corresponding anilines in excellent yields (Scheme 1). The 7-hydroxy-4-methyl coumarin **5a** has been synthesized *via* acid-catalyzed Pechmann condensation between resorcinol and ethyl acetoacetate in 80% yield (Scheme 1). Compounds **6a** and **6b** were prepared by a previously reported method.<sup>[44]</sup> Compounds **5a** and **5b** were treated with propargyl bromide in the presence of K<sub>2</sub>CO<sub>3</sub> as a base in *N,N*-dimethylformamide (DMF) at room temperature, resulting in 4-methyl-7-(prop-2-yn-1-yloxy)-2*H*-chromen-2-one **6a** and 4-(prop-2-yn-1-yloxy)-2*H*-chromen-2-one **6b**, respectively, in excellent yields (Scheme 1).

Finally, the click reaction of compounds **6a,b** with azides **3a–g** in the presence of Cu(OAc)<sub>2</sub> in *t*-BuOH–H<sub>2</sub>O (3:1) at room temperature for 8–10 hr gave the corresponding 1,4-disubstituted-1,2,3-triazole-coumarin conjugates **7a–g** and **8a–g**, respectively, in good-to-excellent yield (88–94%; Scheme 1).

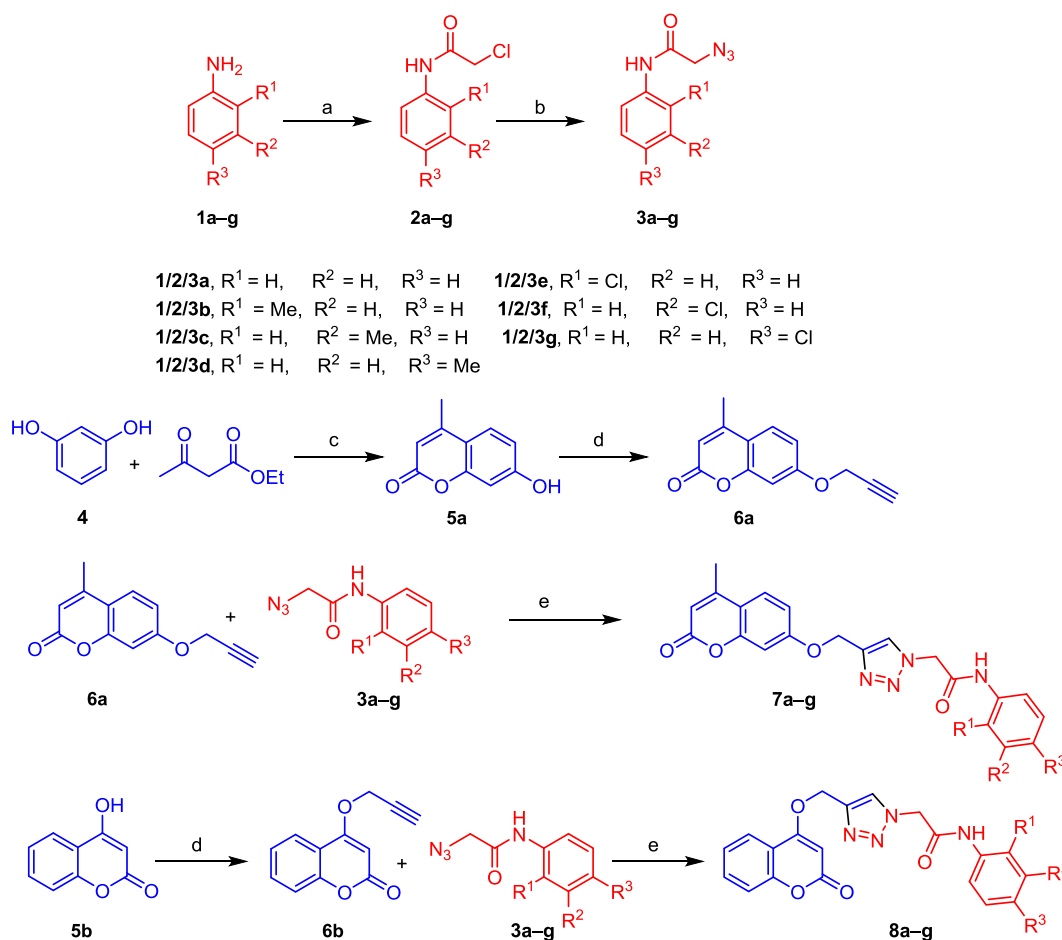
Regioselective formation of 1,4-disubstituted 1,2,3-triazole-coumarin conjugates **7a–g** and **8a–g** has been confirmed by physical

data and spectroscopic techniques such as Fourier-transform infrared spectroscopy (FTIR), <sup>1</sup>H nuclear magnetic resonance (NMR), <sup>13</sup>C NMR, and high-resolution mass spectra (HRMS). According to the FTIR spectrum of compound **7a**, the peaks observed at 3,275 cm<sup>–1</sup> indicate the presence of N–H group, and the peaks observed at 1,698 and 1,670 cm<sup>–1</sup> indicate the presence of two carbonyl groups. In the <sup>1</sup>H NMR spectrum of compound **7a**, the signal at 2.41 ppm indicates the methyl group present on the coumarin ring, and signals at 5.32 and 5.37 ppm are for two protons each and they indicate the presence of two methylene groups attached with nitrogen and oxygen heteroatom, respectively. In addition to this, the signal appearing at 8.32 ppm for one proton clearly indicates the formation of the 1,4-disubstituted 1,2,3-triazole ring. In the <sup>13</sup>C NMR spectrum of compound **7a**, the signal at 18.6 ppm indicates methyl carbon, and the signals at 52.7 and 62.1 ppm indicate the presence of two methylene groups attached to the nitrogen of triazole and oxygen attached to the coumarin ring, respectively. Furthermore, the peak observed at 161.6 ppm indicates amide carbonyl carbon and the peak at 164.6 ppm indicates the presence of carbonyl carbon (lactone carbon) in the coumarin ring. The formation of compound **7a** has been further confirmed by mass spectrometry. The calculated [M+Na]<sup>+</sup> for compound **7a** is at 413.1226, and observed [M+Na]<sup>+</sup> in mass spectrum is at 413.1171. Similarly, compounds **7b–g** and **8a–g** were characterized by the spectral analysis. The structures of synthesized triazole-coumarin conjugates are represented in Figure 4.

### 2.2 | Biological activity

#### 2.2.1 | Antifungal activity

The synthesized compounds were screened for their *in vitro* antifungal activities against five different fungal strains such as *Candida*



**SCHEME 1** The synthesis of coumarin-triazole conjugates. Reagents and conditions: (a) Chloroacetyl chloride, NEt<sub>3</sub>, CH<sub>2</sub>Cl<sub>2</sub>, 0°C at room temperature (rt), 3–5 hr, 85–95%; (b) NaN<sub>3</sub>, toluene, reflux, 5–7 hr, 88–96%; (c) H<sub>2</sub>SO<sub>4</sub>, 0°C, 80%; (d) propargyl bromide, K<sub>2</sub>CO<sub>3</sub>, N,N-dimethylformamide, 2 hr, 93–95%; (e) Cu(OAc)<sub>2</sub> (10 mol%), t-BuOH/H<sub>2</sub>O (3:1), rt, 8–10 hr, 88–94%

*albicans*, *Fusarium oxysporum*, *Aspergillus flavus*, *Aspergillus niger* and *C. neoformans*. The minimum inhibitory concentration (MIC, µg/ml) values of all the newly synthesized compounds were determined by the standard agar dilution method as per the Clinical & Laboratory Standards Institute (CLSI; formerly NCCLS) guidelines.<sup>[56]</sup> Miconazole was used as the standard antifungal drug for the comparison of antifungal activities and dimethyl sulfoxide (DMSO) was used as negative control. The data on the antifungal activity are presented in Table 1. Most of the compounds from the series exhibited a good-to-excellent antifungal activity against all the fungal strains with MIC values ranging from 12.5 to 25 µg/ml.

Without substitution on the phenyl ring, compound 7a exhibited a two fold antifungal activity against *A. niger* and an equipotent activity against *C. albicans* and *F. oxysporum*, with MIC values of 12.5, 25, and 25 µg/ml, respectively, as compared with the standard antifungal drug miconazole. Compound 7b having methyl group at *ortho* position of the phenyl ring was two fold more potent than the standard miconazole against *F. oxysporum*, *A. niger* and *C. neoformans*, with an MIC value of 12.5 µg/ml; it was also equipotent against the fungal strain *C. albicans* with an MIC value of

25 µg/ml. Compound 7c with methyl substituent at *meta* position of the phenyl ring is equipotent to miconazole against fungal strains *A. niger* and *C. neoformans*, with an MIC value of 25 µg/ml, and it is two fold more potent than miconazole against *C. albicans*, with an MIC value of 12.5 µg/ml. Compound 7d with methyl group at *para* position shows two fold potency than the miconazole against *A. niger*, with an MIC value of 12.5 µg/ml, and it is equipotent against *C. albicans* (MIC: 25 µg/ml), *F. oxysporum* (MIC: 25 µg/ml), *A. flavus* (MIC: 12.5 µg/ml), and *C. neoformans* (MIC: 25 µg/ml). Compound 7e (chloro group at *ortho* position) exhibited a two fold activity against *C. albicans* and *A. niger* (MIC: 12.5 µg/ml). Compound 7e also displayed an equivalent activity against *F. oxysporum* and *C. neoformans*, with an MIC value of 25 µg/ml. Compounds 7f and 7g displayed an equipotent activity against *A. niger*, *C. neoformans*, *C. albicans* and *F. oxysporum*, with an MIC value of 25 µg/ml. In addition, compounds 8a–g are equivalent or more potent than the standard miconazole. Among the compounds, 8b, 8c, 8e, and 8f showed an equivalent or two fold activity against all the fungal strains, with MIC values of 12.5–25 µg/ml. The activity results clearly indicate that most of the triazole-coumarin conjugates are

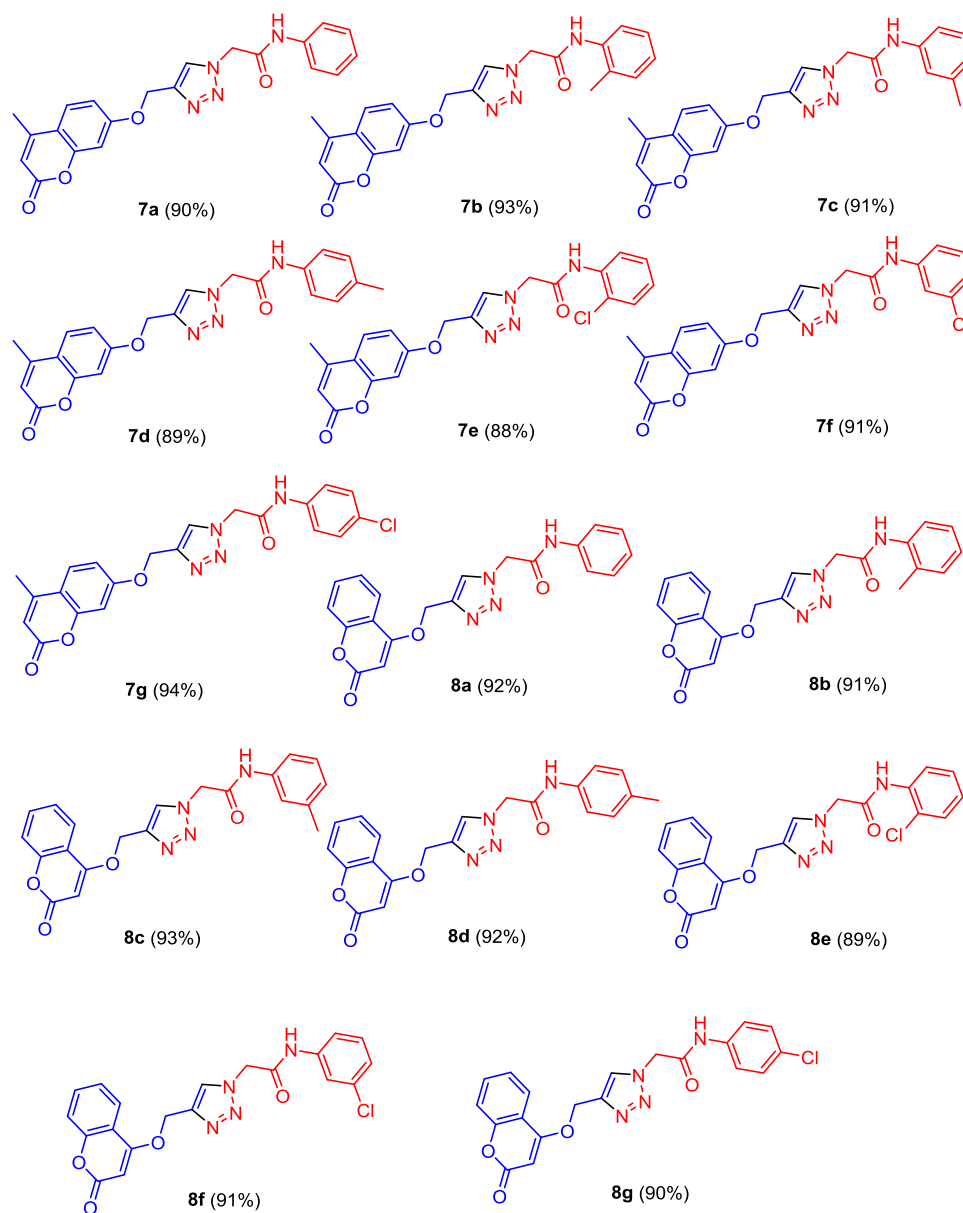


**FIGURE 4** Structures of triazole-coumarin conjugates

more potent or equipotent as compared with the miconazole, as shown in the graphical representation (Figure 5).

## 2.2.2 | Antioxidant activity

The 2,2-diphenyl-1-picrylhydrazyl (DPPH) radical scavenging assay was used to screen the antioxidant activities of the synthesized compounds **7a–g** and **8a–g**. The DPPH radical scavenging assay is the most widely used tool for screening the antioxidant activity of various natural and synthetic compounds. A lower  $IC_{50}$  value indicates more activity against antioxidants. The  $IC_{50}$  (concentration required to scavenge 50% of the radicals) values were calculated to assess the potential antioxidant activities. Butylated hydroxytoluene (BHT) has been used as the standard drug to compare antioxidant activities; the

findings obtained are summarized in Table 1. In comparison to the synthetic antioxidant BHT, compound **7a** exhibited excellent radical scavenging activities, with an  $IC_{50}$  value of  $15.01 \mu\text{g/ml}$ , and remaining compounds showed good-to-moderate activities.

## 2.3 | Computational study

### 2.3.1 | Comparative modeling

The sequence identity and atomic resolution are two key parameters while selection of the template structure, which were 44% and  $2.8 \text{ \AA}$ , respectively, which satisfy the basic criterion for comparative modeling. The final model was subjected to structure validation tool such as Procheck, ProSA, SPDBV and were found that 99.7 percent of the

Compound	Antifungal activity (MIC in $\mu\text{g/ml}$ )					DPPH $\text{IC}_{50}$ ( $\mu\text{g/ml}$ )	Molecular docking score
	CA	FO	AF	AN	CN		
7a	25	25	25	12.5	50	15.01 $\pm$ 0.26	-7.0932
7b	25	12.5	50	12.5	12.5	19.24 $\pm$ 0.19	-7.3901
7c	12.5	50	25	25	25	21.14 $\pm$ 0.97	-6.8629
7d	25	25	12.5	12.5	25	24.37 $\pm$ 0.34	-7.7256
7e	12.5	25	25	12.5	25	38.25 $\pm$ 0.24	-7.9245
7f	50	50	37.5	25	25	29.34 $\pm$ 0.19	-6.8669
7g	25	25	75	75	50	38.18 $\pm$ 0.54	-6.7934
8a	37.5	25	25	37.5	25	36.59 $\pm$ 0.64	-6.2456
8b	12.5	25	12.5	12.5	12.5	27.44 $\pm$ 0.31	-7.1950
8c	25	12.5	25	12.5	25	67.30 $\pm$ 0.05	-6.2411
8d	37.5	25	12.5	75	25	44.31 $\pm$ 0.99	-7.4214
8e	12.5	12.5	12.5	12.5	25	89.32 $\pm$ 0.76	-7.2302
8f	25	12.5	12.5	12.5	25	71.08 $\pm$ 0.26	-6.6233
8g	37.5	50	62.5	37.5	12.5	57.16 $\pm$ 0.79	-6.7248
MA	25	25	12.5	25	25	NA	-5.26
BHT	NA	NA	NA	NA	NA	16.47 $\pm$ 0.18	NA

Abbreviations: AF, *Aspergillus flavus*; AN, *Aspergillus niger*; BHT, butylated hydroxytoluene; CA, *Candida albicans*; CN, *Cryptococcus neoformans*; DPPH, 2,2-diphenyl-1-picrylhydrazyl; FO, *Fusarium oxysporum*; MA, miconazole; MIC, minimum inhibitory concentration; NA, not applicable.

residue followed in the allowed region. Also, overall model quality was assessed using Prosa where Z score is -3.2 and  $\text{C}\alpha$  deviation is 0.45 Å, respectively. The validation study of the model suggested that it was perfect for further computation study.

### 2.3.2 | Molecular docking study

The molecular docking study of all synthesized triazole-coumarin conjugates, 7a-g and 8a-g, was performed against modeled

three-dimensional structure of cytochrome P450 lanosterol 14 $\alpha$ -demethylase of *C. albicans* to understand the binding affinity and binding interactions of enzyme and synthesized derivatives. The synthesized triazole-coumarin conjugates (7a-g, 8a-g) and the standard drug miconazole were docked in the active site of modeled CACYP51 using the AutoDock Vina docking tool. The results of docking are shown in Table 1. The analysis of docking interaction revealed that the triazole ring was mainly responsible for the interaction.

The triazole-coumarin conjugates 7b, 7d, 7e, 8b and 8e reproduced a similar result as that of in vitro activity data. All active

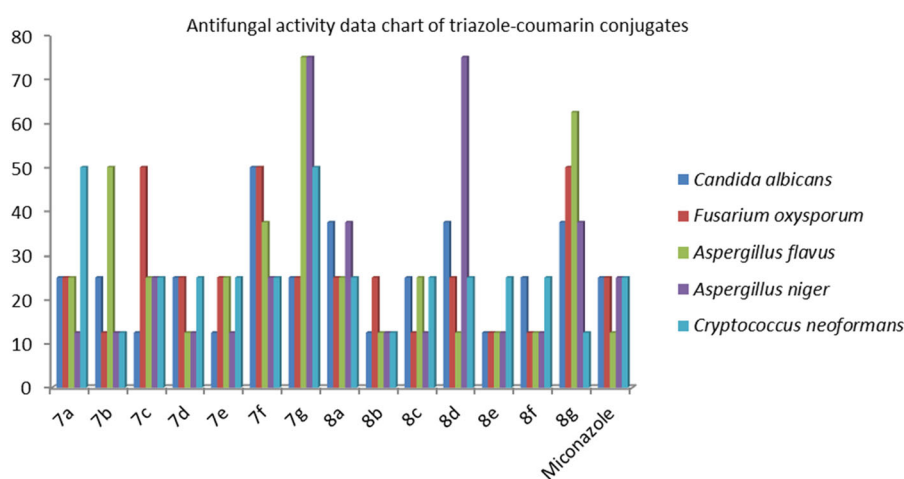


**TABLE 1** In vitro biological evaluation of the synthesized triazole-coumarin conjugates 7a-g and 8a-g

**FIGURE 5** A comparison of the antifungal activities of triazole-coumarin conjugates with miconazole



compounds efficiently interact with the active-site residues like Tyr105, Phe108, Phe121, Val130, Tyr168, Tyr154, Phe162, Leu412, Phe246, Met342, Ala343, Cys439, Ser414, Leu412 and Met544. The triazole-coumarin conjugates having *ortho* substitution on the phenyl ring partially replicate in vitro antifungal results, that is, **8b** and **8e**.

The *ortho*-substituted ( $-CH_3$ ) phenyl ring derivative **8b** (-7.19) interacts with polar and nonpolar amino acids of the active site. The polar amino acid Ser414 interacts with the nitrogen atom of the triazole ring to form conventional hydrogen bond interactions with a distance of 2.37 Å. The sulfur atom of polar amino acid Cys439 interacts with  $\pi$  electron cloud of the phenyl ring to form  $\pi$ -sulfur interactions. The aliphatic and hydrophobic amino acids Leu412, Tyr105, Phe108, Phe121, and Val130 interact with  $\pi$  electron cloud of aromatic ring to form  $\pi$ - $\pi$  T-shaped,  $\pi$ - $\pi$  stacked, and  $\pi$ -sulfur interactions with various distance values shown in Figure 6a.

The *ortho*-substituted ( $-Cl$ ) phenyl ring derivative **8e** (-7.23) interacts with aliphatic and hydrophobic amino acid residues Ala342 and Tyr168, where it interacts with carbonyl oxygen atom and nitrogen atom of the triazole ring with a distance of 2.21 and 2.08 Å to form conventional hydrogen bond interactions. The polar amino acid residue Met342 and hydrophobic amino acid Phe264 form a carbon-hydrogen bond and  $\pi$  interaction with *ortho*-substituted

chlorine atom with a distance of 2.08 and 3.77 Å. However, aliphatic and hydrophobic amino acids Leu412, Phe264, Phe162, Tyr154, and Met342 interact with  $\pi$  electron cloud of aromatic phenyl rings to form  $\pi$ - $\pi$  stacked, amide- $\pi$  stacked, alkyl and  $\pi$ -alkyl interactions shown in Figure 6b.

### 2.3.3 | In silico ADME prediction

Early prediction of druglikeness properties of lead compounds is an important task, as it decides the time and cost of drug discovery and development. Many of the active agents with a significant biological activity have failed in clinical trials due to inadequate druglikeness properties.<sup>[57]</sup> The druglikeness properties were predicted by analyzing ADME parameters based on Lipinski's rule of five. We had calculated and analyzed various physical descriptors and pharmaceutical relevant properties for ADMET prediction by using FAFDrugs2, and data are summarized in Table 2.

All the compounds showed significant values for the various parameters analyzed and showed good drug-like characteristics based on Lipinski's rule of five and its variants that characterized these agents to be likely orally active. The data obtained for all the

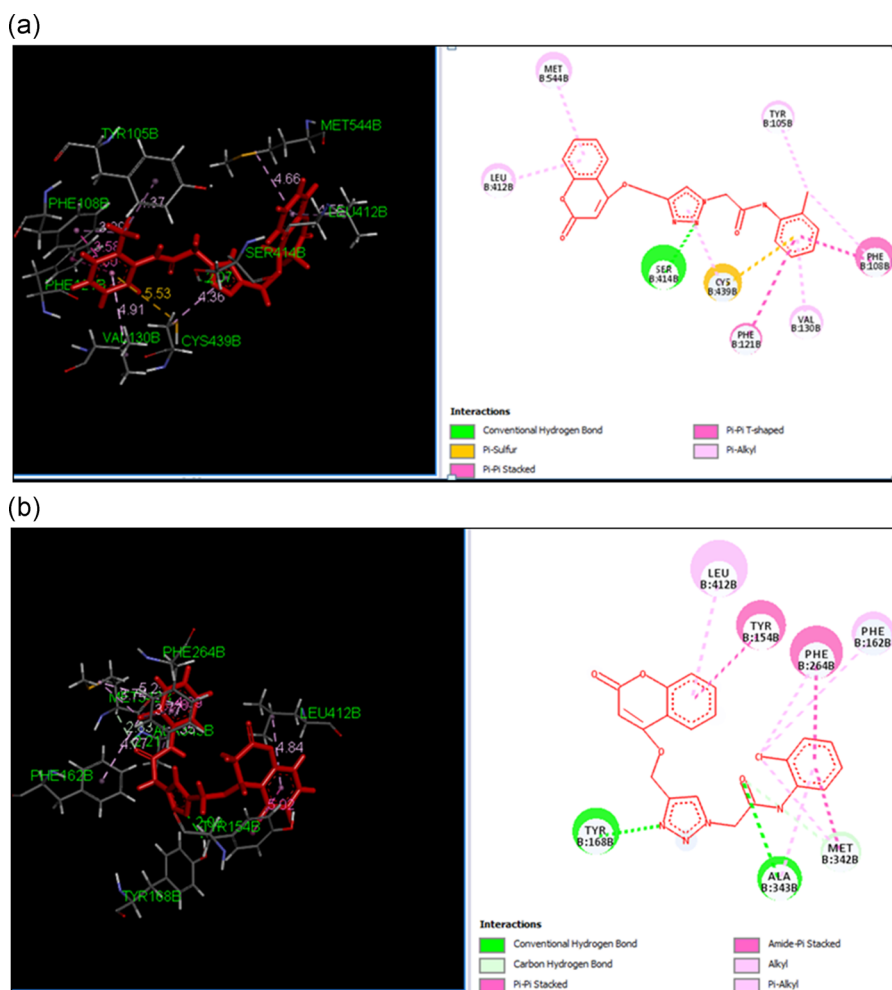


**FIGURE 6** Binding pose and molecular interactions of (a) **8b** and (b) **8e** in the active site of cytochrome P450 lanosterol 14 $\alpha$ -demethylase (CYP51)

**TABLE 2** Pharmacokinetic parameters of triazole-coumarin conjugates (**7a-g** and **8a-g**)

Entry	%ABS	MW	LogP	PSA	RotB	RigidB	HBD	HBA	Ratio H/C	Lipinski violation	Toxicity
<b>7a</b>	74.76	390.39	2.98	99.25	6	25	1	6	0.4	0	Nontoxic
<b>7b</b>	74.76	404.42	3.29	99.25	6	25	1	6	0.4	0	Nontoxic
<b>7c</b>	74.76	404.42	3.29	99.25	6	25	1	6	0.4	0	Nontoxic
<b>7d</b>	74.76	404.42	3.29	99.25	6	25	1	6	0.4	0	Nontoxic
<b>7e</b>	74.76	424.84	3.64	99.25	6	25	1	6	0.4	0	Nontoxic
<b>7f</b>	74.76	424.84	3.64	99.25	6	25	1	6	0.4	0	Nontoxic
<b>7g</b>	74.76	424.84	3.64	99.25	6	25	1	6	0.4	0	Nontoxic
<b>8a</b>	76.11	378.38	2.56	95.34	6	25	1	6	0.4	0	Nontoxic
<b>8b</b>	76.11	392.41	2.87	95.34	6	25	1	6	0.4	0	Nontoxic
<b>8c</b>	76.11	392.41	2.87	95.34	6	25	1	6	0.4	0	Nontoxic
<b>8d</b>	76.11	392.41	2.87	95.34	6	25	1	6	0.4	0	Nontoxic
<b>8e</b>	76.11	412.83	3.21	95.34	6	25	1	6	0.5	0	Nontoxic
<b>8f</b>	76.11	412.83	3.21	95.34	6	25	1	6	0.5	0	Nontoxic
<b>8g</b>	76.11	412.83	3.21	95.34	6	25	1	6	0.5	0	Nontoxic

Abbreviations: HBA, hydrogen bond acceptor; HBD, hydrogen bond donor; MW, molecular weight; PSA, polar surface area; RotB, rotatable bonds; RigidB, rigid bonds; %ABS, percentage absorption.

synthesized compounds were within the range of accepted values. None of the synthesized compounds had violated the Lipinski's rule of five. The value of polar surface area, logP, and H/C ratio of synthesized compounds **7a-g** and **8a-g** indicated good oral bioavailability. The parameters like the number of rotatable bonds and number of rigid bonds are linked with the intestinal absorption; results showed that all synthesized compounds had good absorption. All the synthesized compounds were found to be nontoxic. The in silico assessment of all the synthetic compounds has shown that they have very good pharmacokinetic properties, which is reflected in their physicochemical values, thus ultimately enhancing pharmacological properties of these molecules.

### 3 | CONCLUSIONS

In conclusion, we have synthesized new triazole-coumarin conjugates via the click chemistry approach, which were evaluated for their in vitro antifungal and antioxidant activity. The synthesized compounds displayed a promising antifungal activity as compared with the standard drug miconazole. Compounds **7b**, **7d**, **7e**, **8b**, and **8e** displayed an excellent antifungal activity as compared with the standard antifungal drug miconazole. Compound **7a** displayed a potential antioxidant activity when compared with standard BHT. In addition, molecular docking study of these synthesized triazole-coumarin conjugates reveals that they have a high affinity toward the active site of enzyme P450 cytochrome lanosterol 14 $\alpha$ -demethylase, which offers a strong platform for new structure-based design efforts. Furthermore, the analysis of the ADME parameters for the synthesized compounds predicted good drug-like properties and potential for development as

oral drug candidates. Thus, we suggest that compounds **7a** (antioxidant activity), **7b**, **7d**, **7e**, **8b** and **8e** (antifungal activity) can be developed as an important lead moiety, as they replicate in vitro activity in the inhibition assay and in silico molecular docking study. They can be used in scaffolds, hoping for the design and development of new lead compounds as antifungal agents.

## 4 | EXPERIMENTAL

### 4.1 | Chemistry

#### 4.1.1 | General

All the solvents and reagents were purchased from commercial suppliers, Sigma-Aldrich, Rankem India Ltd., and Spectrochem Pvt. Ltd., and were used without further purification. The completion of the reactions was monitored by thin-layer chromatography (TLC) on aluminum plates coated with silica gel 60 F<sub>254</sub>, with 0.25 mm thickness (Merck). The detection of the components was done by exposure to iodine vapors or UV light. Melting points were determined by open capillary methods and were uncorrected. <sup>1</sup>H NMR and <sup>13</sup>C NMR spectra were recorded in DMSO-*d*<sub>6</sub> on a Bruker DRX-400 and 500-MHz spectrometer. Infrared (IR) spectra were recorded using a Bruker ALPHA Eco-ATR FTIR spectrometer. High-resolution mass spectra (HRMS) were recorded on an Agilent 6520 (QTOF) mass spectrometer.

The original spectra of the investigated compounds, together with their InChI codes and some biological activity data, are provided as Supporting Information Data.



#### 4.1.2 | General procedure for the synthesis of substituted 2-(4-((4-methyl-2-oxo-2H-chromen-7-yl)-oxy)methyl)-1H-1,2,3-triazol-1-yl)-N-phenylacetamide derivatives 7a–g and 8a–g

To the stirred solution of alkyne **6** (1 mmol), azide **3** (1 mmol) and copper diacetate ( $\text{Cu}(\text{OAc})_2$ ; 10 mol%) in  $t\text{-BuOH-H}_2\text{O}$  (3:1) were added, and the resulting mixture was stirred at room temperature for 8–10 hr. The progress of the reaction was monitored by TLC using ethyl acetate/hexane as a solvent system. The reaction mixture was quenched with crushed ice, and the obtained solid was filtered and washed with water. The crude solid was crystallized in ethanol to afford the corresponding pure product. The synthesized compounds **7a–g** and **8a–g** were characterized by IR,  $^1\text{H}$  NMR,  $^{13}\text{C}$  NMR, and mass spectroscopy.

##### 2-(4-((4-Methyl-2-oxo-2H-chromen-7-yl)oxy)methyl)-1H-1,2,3-triazol-1-yl)-N-phenylacetamide (7a)

Compound **7a** was obtained via the 1,3-dipolar cycloaddition reaction between azide **3a** and alkyne **6a** in 8.5 hr as a white solid, mp: 149–151°C; FTIR ( $\text{cm}^{-1}$ ): 3,275 (N–H stretching), 1,698 and 1,670 (C=O stretching);  $^1\text{H}$  NMR (500 MHz,  $\text{DMSO-}d_6$ ,  $\delta$  ppm): 2.41 (s, 3H,  $-\text{CH}_3$ ), 5.32 (s, 2H,  $-\text{NCH}_2\text{CO-}$ ), 5.37 (s, 2H,  $-\text{OCH}_2$ ), 6.23 (s, 1H, Ar-H), 7.07 (dd,  $J = 8.0, 3.0$  Hz, 1H, Ar-H), 7.10 (d,  $J = 8.0$  Hz, 1H, Ar-H), 7.18 (s, 1H, Ar-H), 7.34 (t,  $J = 8.0$  Hz, 2H, Ar-H), 7.58 (d,  $J = 8.0$  Hz, 2H, Ar-H), 7.71 (d,  $J = 8.0$  Hz, 1H, Ar-H), 8.32 (s, 1H, triazole), and 10.48 (s, 1H, NH);  $^{13}\text{C}$  NMR (125 MHz,  $\text{DMSO-}d_6$ ,  $\delta$  ppm): 18.6, 52.7, 62.1, 102.1, 111.8, 113.1, 113.9, 119.7, 124.3, 127.0, 127.1, 129.4, 138.9, 142.3, 153.9, 155.2, 160.6, 161.6, and 164.6; mass calculated for  $\text{C}_{21}\text{H}_{18}\text{N}_4\text{O}_4\text{Na}$  [ $\text{M}+\text{Na}$ ] $^+$ : 413.1226 and found: 413.1171.

##### 2-(4-((4-Methyl-2-oxo-2H-chromen-7-yl)oxy)methyl)-1H-1,2,3-triazol-1-yl)-N-(o-tolyl)acetamide (7b)

Compound **7b** was obtained via the 1,3-dipolar cycloaddition reaction between azide **3b** and alkyne **6a** in 9.5 hr as an orange solid, mp: 195–197°C; FTIR ( $\text{cm}^{-1}$ ): 3,276 (N–H stretching), 1,690 and 1,670 (C=O stretching);  $^1\text{H}$  NMR (400 MHz,  $\text{DMSO-}d_6$ ,  $\delta$  ppm): 1.95 (s, 3H,  $-\text{CH}_3$ ), 2.12 (s, 3H,  $-\text{CH}_3$ ), 5.04 (s, 4H,  $-\text{NCH}_2\text{CO-}$  and  $-\text{OCH}_2$ ), 5.84 (s, 1H, Ar-H), 6.67–6.68 (m, 4H, Ar-H), 7.25 (s, 3H, Ar-H), 7.75 (s, 1H, triazole), and 9.07 (s, 1H, NH); mass calculated for  $\text{C}_{22}\text{H}_{20}\text{N}_4\text{O}_4\text{Na}$  [ $\text{M}+\text{Na}$ ] $^+$ : 427.1382 and found: 427.1334.

##### 2-(4-((4-Methyl-2-oxo-2H-chromen-7-yl)oxy)methyl)-1H-1,2,3-triazol-1-yl)-N-(m-tolyl)acetamide (7c)

Compound **7c** was obtained via the 1,3-dipolar cycloaddition reaction between azide **3c** and alkyne **6a** in 8 hr as a white solid, mp: 190–192°C; FTIR ( $\text{cm}^{-1}$ ): 3,291 (N–H stretching), 1,678 (C=O stretching);  $^1\text{H}$  NMR (500 MHz,  $\text{DMSO-}d_6$ ,  $\delta$  ppm): 2.27 (s, 3H,  $-\text{CH}_3$ ), 2.39 (s, 3H,  $-\text{CH}_3$ ), 5.31 (s, 2H,  $-\text{NCH}_2\text{CO-}$ ), 5.36 (s, 2H,  $-\text{OCH}_2$ ), 6.21 (s, 1H, Ar-H), 6.91 (d,  $J = 8.0$  Hz, 1H, Ar-H), 7.05 (dd,  $J = 8.0, 4.0$  Hz, 1H, Ar-H), 7.17 (d,  $J = 4.0$  Hz, 1H, Ar-H), 7.21 (t,  $J = 8.0$  Hz, 1H, Ar-H), 7.37 (d,  $J = 8.0$  Hz, 1H, Ar-H), 7.42 (s, 1H, Ar-H), 7.69 (d,  $J = 8.0$  Hz, 1H, Ar-H), 8.31 (s, 1H, triazole) and 10.40 (s, 1H, NH);  $^{13}\text{C}$  NMR (125 MHz,  $\text{DMSO-}d_6$ ,  $\delta$  ppm): 17.9, 20.9, 52.1, 61.4, 101.4,

111.1, 112.4, 113.2, 116.3, 119.6, 124.3, 126.3, 126.4, 128.6, 138.0, 138.1, 141.6, 153.2, 154.5, 160.0, 160.9, and 163.9; HRMS calculated for  $\text{C}_{22}\text{H}_{21}\text{N}_4\text{O}_4$  [ $\text{M}+\text{H}$ ] $^+$ : 405.1563 and found: 405.1571.

##### 2-(4-((4-Methyl-2-oxo-2H-chromen-7-yl)oxy)methyl)-1H-1,2,3-triazol-1-yl)-N-(p-tolyl)acetamide (7d)

Compound **7d** was obtained via the 1,3-dipolar cycloaddition reaction between azide **3d** and alkyne **6a** in 9 hr as a red solid, mp: 216–218°C; FTIR ( $\text{cm}^{-1}$ ): 3,248 (N–H stretching), 1,698 and 1,659 (C=O stretching);  $^1\text{H}$  NMR (400 MHz,  $\text{DMSO-}d_6$ ,  $\delta$  ppm): 2.25 (s, 3H,  $-\text{CH}_3$ ), 2.40 (s, 3H,  $-\text{CH}_3$ ), 5.31 (s, 2H,  $-\text{NCH}_2\text{CO-}$ ), 5.34 (s, 2H,  $-\text{OCH}_2$ ), 6.22 (s, 1H, Ar-H), 7.06 (dd,  $J = 8.0, 4.0$  Hz, 1H, Ar-H), 7.13 (d,  $J = 8.0$  Hz, 2H, Ar-H), 7.17 (d,  $J = 4.0$  Hz, 1H, Ar-H), 7.46 (d,  $J = 8.0$  Hz, 2H, Ar-H), 7.70 (d,  $J = 8.0$  Hz, 1H, Ar-H), 8.31 (s, 1H, triazole), and 10.40 (s, 1H, NH);  $^{13}\text{C}$  NMR (100 MHz,  $\text{DMSO-}d_6$ ,  $\delta$  ppm): 18.5, 20.8, 52.5, 61.9, 101.9, 111.6, 113.0, 113.7, 119.6, 126.9, 127.0, 129.6, 133.1, 136.2, 142.1, 153.8, 155.0, 160.5, 161.4, and 164.2; HRMS calculated for  $\text{C}_{22}\text{H}_{19}\text{N}_4\text{O}_4$  [ $\text{M}-\text{H}$ ] $^+$ : 403.1412 and found: 403.1424.

##### N-(2-Chlorophenyl)-2-(4-((4-methyl-2-oxo-2H-chromen-7-yl)oxy)methyl)-1H-1,2,3-triazol-1-yl)acetamide (7e)

Compound **7e** was obtained via the 1,3-dipolar cycloaddition reaction between azide **3e** and alkyne **6a** in 9.5 hr as a white solid, mp: 206–208°C; FTIR ( $\text{cm}^{-1}$ ): 3,118 (N–H stretching), 1,664 and 1,600 (C=O stretching);  $^1\text{H}$  NMR (400 MHz,  $\text{DMSO-}d_6$ ,  $\delta$  ppm): 2.40 (s, 3H,  $-\text{CH}_3$ ), 5.31 (s, 2H,  $-\text{NCH}_2\text{CO-}$ ), 5.48 (s, 2H,  $-\text{OCH}_2$ ), 6.22 (s, 1H, Ar-H), 7.05 (d,  $J = 8.0$  Hz, 1H, Ar-H), 7.17 (s, 1H, Ar-H), 7.22 (t,  $J = 8.0$  Hz, 1H, Ar-H), 7.34 (t,  $J = 8.0$  Hz, 1H, Ar-H), 7.52 (d,  $J = 8.0$  Hz, 1H, Ar-H), 7.69 (d,  $J = 8.0$  Hz, 1H, Ar-H), 7.74 (d,  $J = 8.0$  Hz, 1H, Ar-H), 8.32 (s, 1H, triazole), and 10.09 (s, 1H, NH);  $^{13}\text{C}$  NMR (100 MHz,  $\text{DMSO-}d_6$ ,  $\delta$  ppm): 18.1, 52.0, 61.6, 101.6, 111.3, 112.6, 113.4, 125.9, 126.3, 126.5, 126.7, 126.8, 127.6, 129.6, 134.1, 141.8, 153.4, 154.7, 160.1, 161.1, and 164.9; HRMS calculated for  $\text{C}_{21}\text{H}_{16}\text{ClN}_4\text{O}_4$  [ $\text{M}-\text{H}$ ] $^+$ : 423.0866 and found: 423.0880.

##### N-(3-Chlorophenyl)-2-(4-((4-methyl-2-oxo-2H-chromen-7-yl)oxy)methyl)-1H-1,2,3-triazol-1-yl)acetamide (7f)

Compound **7f** was obtained via the 1,3-dipolar cycloaddition reaction between azide **3f** and alkyne **6a** in 10 hr as a yellow solid, mp: 218–220°C;  $^1\text{H}$  NMR (400 MHz,  $\text{DMSO-}d_6$ ,  $\delta$  ppm): 2.39 (s, 3H,  $-\text{CH}_3$ ), 5.31 (s, 2H,  $-\text{NCH}_2\text{CO-}$ ), 5.38 (s, 2H,  $-\text{OCH}_2$ ), 6.21 (s, 1H, Ar-H), 7.05 (dd,  $J = 8.0, 4.0$  Hz, 1H, Ar-H), 7.15 (d,  $J = 8.0$  Hz, 2H, Ar-H), 7.36 (t,  $J = 8.0$  Hz, 1H, Ar-H), 7.44 (d,  $J = 8.0$  Hz, 1H, Ar-H), 7.69 (d,  $J = 8.0$  Hz, 1H, Ar-H), 7.77 (s, 1H, Ar-H), 8.31 (s, 1H, triazole), and 10.68 (s, 1H, NH);  $^{13}\text{C}$  NMR (100 MHz,  $\text{DMSO-}d_6$ ,  $\delta$  ppm): 18.2, 52.2, 61.6, 101.6, 111.3, 112.6, 113.4, 117.7, 118.8, 123.6, 126.5, 126.7, 130.7, 133.2, 139.8, 141.8, 154.7, 160.2, 161.1, and 164.7; HRMS calculated for  $\text{C}_{21}\text{H}_{16}\text{ClN}_4\text{O}_4$  [ $\text{M}-\text{H}$ ] $^+$ : 423.0866 and found: 423.0872.

##### N-(4-Chlorophenyl)-2-(4-((4-methyl-2-oxo-2H-chromen-7-yl)oxy)methyl)-1H-1,2,3-triazol-1-yl)acetamide (7g)

Compound **7g** was obtained via the 1,3-dipolar cycloaddition reaction between azide **3g** and alkyne **6a** in 8.5 hr as a yellow solid,

mp: 210–212°C;  $^1\text{H}$  NMR (400 MHz, DMSO- $d_6$ ,  $\delta$  ppm): 2.40 (s, 3H,  $-\text{CH}_3$ ), 5.30 (s, 2H,  $-\text{NCH}_2\text{CO}-$ ), 5.36 (s, 2H,  $-\text{OCH}_2$ ), 6.23 (s, 1H, Ar-H), 7.05 (dd,  $J = 8.0, 4.0$  Hz, 1H, Ar-H), 7.17 (d,  $J = 4.0$  Hz, 1H, Ar-H), 7.39 (d,  $J = 8.0$  Hz, 2H, Ar-H), 7.60 (d,  $J = 8.0$  Hz, 2H, Ar-H), 7.70 (d,  $J = 8.0$  Hz, 1H, Ar-H), 8.31 (s, 1H, triazole), and 10.63 (s, 1H, NH); HRMS calculated for  $\text{C}_{21}\text{H}_{16}\text{ClN}_4\text{O}_4$   $[\text{M}-\text{H}]^+$ : 423.0866 and found: 423.0878.

2-(4-[[[2-Oxo-2H-chromen-4-yl]oxy]methyl]-1H-1,2,3-triazol-1-yl)-N-phenylacetamide (**8a**)

Compound **8a** was obtained via the 1,3-dipolar cycloaddition reaction between azide **3a** and alkyne **6b** in 10 hr as a white solid, mp: 216–218°C;  $^1\text{H}$  NMR (400 MHz, DMSO- $d_6$ ,  $\delta$  ppm): 5.40 (s, 2H,  $-\text{NCH}_2\text{CO}-$ ), 5.47 (s, 2H,  $-\text{OCH}_2$ ), 6.20 (s, 1H, Ar-H), 7.09 (t,  $J = 8.0$  Hz, 1H, Ar-H), 7.33 (t,  $J = 8.0$  Hz, 3H, Ar-H), 7.40 (d,  $J = 8.0$  Hz, 1H, Ar-H), 7.59 (d,  $J = 8.0$  Hz, 2H, Ar-H), 7.65 (t,  $J = 8.0$  Hz, 1H, Ar-H), 7.74 (d,  $J = 8.0$  Hz, 1H, Ar-H), 8.43 (s, 1H, triazole), and 10.51 (s, 1H, NH);  $^{13}\text{C}$  NMR (100 MHz, DMSO- $d_6$ ,  $\delta$  ppm): 52.3, 62.8, 91.4, 115.1, 116.5, 119.3, 122.8, 123.8, 124.3, 127.1, 128.9, 132.8, 138.4, 152.8, 164.2, and 164.4; HRMS calculated for  $\text{C}_{20}\text{H}_{15}\text{N}_4\text{O}_4$   $[\text{M}-\text{H}]^+$ : 375.1099 and found: 375.1080.

2-(4-[[[2-Oxo-2H-chromen-4-yl]oxy]methyl]-1H-1,2,3-triazol-1-yl)-N-(o-tolyl)acetamide (**8b**)

Compound **8b** was obtained via the 1,3-dipolar cycloaddition reaction between azide **3b** and alkyne **6b** in 8.5 hr as a white solid, mp: 170–172°C; FTIR ( $\text{cm}^{-1}$ ): 3,248 (N–H stretching), 1,698 and 1,659 ( $\text{C}=\text{O}$  stretching);  $^1\text{H}$  NMR (400 MHz, DMSO- $d_6$ ,  $\delta$  ppm): 2.24 (s, 3H,  $-\text{CH}_3$ ), 5.45 (s, 2H,  $-\text{NCH}_2\text{CO}-$ ), 5.47 (s, 2H,  $-\text{OCH}_2$ ), 6.20 (s, 1H, Ar-H), 7.11 (t,  $J = 8.0$  Hz, 1H, Ar-H), 7.17 (t,  $J = 8.0$  Hz, 1H, Ar-H), 7.23 (d,  $J = 8.0$  Hz, 1H, Ar-H), 7.33 (t,  $J = 8.0$  Hz, 1H, Ar-H), 7.42 (d,  $J = 8.0$  Hz, 2H, Ar-H), 7.65 (t,  $J = 8.0$  Hz, 1H, Ar-H), 7.73 (d,  $J = 8.0$  Hz, 1H, Ar-H), 8.43 (s, 1H, triazole), and 9.83 (s, 1H, NH);  $^{13}\text{C}$  NMR (100 MHz, DMSO- $d_6$ ,  $\delta$  ppm): 17.8, 52.0, 62.8, 91.4, 115.1, 116.5, 122.8, 124.2, 124.8, 125.6, 126.1, 127.0, 130.5, 131.6, 132.8, 135.5, 152.8, 161.6, 164.3, and 164.4; HRMS calculated for  $\text{C}_{21}\text{H}_{17}\text{N}_4\text{O}_4$   $[\text{M}-\text{H}]^+$ : 389.1255 and found: 389.1311.

2-(4-[[[2-Oxo-2H-chromen-4-yl]oxy]methyl]-1H-1,2,3-triazol-1-yl)-N-(m-tolyl)acetamide (**8c**)

Compound **8c** was obtained via the 1,3-dipolar cycloaddition reaction between azide **3c** and alkyne **6b** in 9 hr as a yellow solid, mp: 211–213°C; FTIR ( $\text{cm}^{-1}$ ): 3,307 (N–H stretching), 1,703 and 1,666 ( $\text{C}=\text{O}$  stretching);  $^1\text{H}$  NMR (400 MHz, DMSO- $d_6$ ,  $\delta$  ppm): 2.27 (s, 3H,  $-\text{CH}_3$ ), 5.40 (s, 2H,  $-\text{NCH}_2\text{CO}-$ ), 5.47 (s, 2H,  $-\text{OCH}_2$ ), 6.20 (s, 1H, Ar-H), 6.90 (d,  $J = 8.0$  Hz, 1H, Ar-H), 7.21 (t,  $J = 8.0$  Hz, 1H, Ar-H), 7.30–7.44 (m, 4H, Ar-H), 7.65 (t,  $J = 8.0$  Hz, 1H, Ar-H), 7.73 (d,  $J = 8.0$  Hz, 1H, Ar-H), 8.43 (s, 1H, triazole) and 10.44 (s, 1H, NH);  $^{13}\text{C}$  NMR (125 MHz, DMSO- $d_6$ ,  $\delta$  ppm): 21.4, 52.5, 63.0, 91.6, 115.3, 116.6, 116.7, 120.0, 123.3, 124.4, 124.7, 127.3, 129.0, 133.0, 138.4, 138.5, 153.0, 161.8, 164.3, and 164.6; HRMS calculated for  $\text{C}_{21}\text{H}_{17}\text{N}_4\text{O}_4$   $[\text{M}-\text{H}]^+$ : 389.1255 and found: 389.1346.

2-(4-[[[2-Oxo-2H-chromen-4-yl]oxy]methyl]-1H-1,2,3-triazol-1-yl)-N-(p-tolyl)acetamide (**8d**)

Compound **8d** was obtained via the 1,3-dipolar cycloaddition reaction between azide **3d** and alkyne **6b** in 8.5 hr as a white solid, mp: 247–249°C;  $^1\text{H}$  NMR (400 MHz, DMSO- $d_6$ ,  $\delta$  ppm): 2.25 (s, 3H,  $-\text{CH}_3$ ), 5.38 (s, 2H,  $-\text{NCH}_2\text{CO}-$ ), 5.47 (s, 2H,  $-\text{OCH}_2$ ), 6.20 (s, 1H, Ar-H), 7.13 (d,  $J = 8.0$  Hz, 2H, Ar-H), 7.34 (t,  $J = 8.0$  Hz, 1H, Ar-H), 7.41 (d,  $J = 8.0$  Hz, 1H, Ar-H), 7.47 (d,  $J = 8.0$  Hz, 2H, Ar-H), 7.66 (t,  $J = 8.0$  Hz, 1H, Ar-H), 7.74 (d,  $J = 8.0$  Hz, 1H, Ar-H), 8.41 (s, 1H, triazole), and 10.41 (s, 1H, NH);  $^{13}\text{C}$  NMR (100 MHz, DMSO- $d_6$ ,  $\delta$  ppm): 20.5, 52.3, 62.8, 91.4, 116.5, 119.2, 122.8, 124.2, 127.0, 129.3, 132.8, 135.9, 140.6, 152.8, 161.6, 163.9, and 164.4; HRMS calculated for  $\text{C}_{21}\text{H}_{17}\text{N}_4\text{O}_4$   $[\text{M}-\text{H}]^+$ : 389.1255 and found: 389.1314.

N-(2-Chlorophenyl)-2-(4-[[[2-oxo-2H-chromen-4-yl]oxy]methyl]-1H-1,2,3-triazol-1-yl)acetamide (**8e**)

Compound **8e** was obtained via the 1,3-dipolar cycloaddition reaction between azide **3e** and alkyne **6b** in 9.5 hr as a brown solid, mp: 217–219°C; FTIR ( $\text{cm}^{-1}$ ): 3,254 (N–H stretching), 1,709 and 1,673 ( $\text{C}=\text{O}$  stretching);  $^1\text{H}$  NMR (400 MHz, DMSO- $d_6$ ,  $\delta$  ppm): 5.47 (s, 2H,  $-\text{NCH}_2\text{CO}-$ ), 5.51 (s, 2H,  $-\text{OCH}_2$ ), 6.19 (s, 1H, Ar-H), 7.20–7.76 (m, 8H, Ar-H), 8.43 (s, 1H, triazole), and 10.12 (s, 1H, NH);  $^{13}\text{C}$  NMR (100 MHz, DMSO- $d_6$ ,  $\delta$  ppm): 52.0, 62.7, 91.4, 115.0, 116.5, 122.8, 124.2, 125.9, 126.3, 126.8, 127.1, 127.6, 129.6, 132.8, 134.1, 152.8, 161.5, 164.3, and 164.8; HRMS calculated for  $\text{C}_{20}\text{H}_{14}\text{ClN}_4\text{O}_4$   $[\text{M}-\text{H}]^+$ : 409.0709 and found: 409.0722.

N-(3-Chlorophenyl)-2-(4-[[[2-oxo-2H-chromen-4-yl]oxy]methyl]-1H-1,2,3-triazol-1-yl)acetamide (**8f**)

Compound **8f** was obtained via the 1,3-dipolar cycloaddition reaction between azide **3f** and alkyne **6b** in 10 hr as a red solid, mp: 218–220°C;  $^1\text{H}$  NMR (400 MHz, DMSO- $d_6$ ,  $\delta$  ppm): 5.42 (s, 2H,  $-\text{NCH}_2\text{CO}-$ ), 5.47 (s, 2H,  $-\text{OCH}_2$ ), 6.20 (s, 1H, Ar-H), 7.15 (d,  $J = 8.0$  Hz, 1H, Ar-H), 7.32–7.41 (m, 3H, Ar-H), 7.45 (d,  $J = 8.0$  Hz, 1H, Ar-H), 7.65 (t,  $J = 8.0$  Hz, 1H, Ar-H), 7.73 (d,  $J = 8.0$  Hz, 1H, Ar-H), 7.78 (s, 1H, Ar-H), 8.43 (s, 1H, triazole), and 10.71 (s, 1H, NH);  $^{13}\text{C}$  NMR (100 MHz, DMSO- $d_6$ ,  $\delta$  ppm): 52.3, 62.8, 91.4, 115.1, 116.5, 117.7, 118.8, 122.8, 123.6, 124.2, 127.0, 130.7, 132.8, 133.2, 139.8, 140.8, 152.8, 161.6, 164.4, and 164.6; HRMS calculated for  $\text{C}_{20}\text{H}_{14}\text{ClN}_4\text{O}_4$   $[\text{M}-\text{H}]^+$ : 409.0709 and found: 409.0724.

N-(4-Chlorophenyl)-2-(4-[[[2-oxo-2H-chromen-4-yl]oxy]methyl]-1H-1,2,3-triazol-1-yl)acetamide (**8g**)

Compound **8g** was obtained via the 1,3-dipolar cycloaddition reaction between azide **3g** and alkyne **6b** in 8 hr as a white solid, mp: 240–242°C;  $^1\text{H}$  NMR (400 MHz, DMSO- $d_6$ ,  $\delta$  ppm): 5.40 (s, 2H,  $-\text{NCH}_2\text{CO}-$ ), 5.46 (s, 2H,  $-\text{OCH}_2$ ), 6.19 (s, 1H, Ar-H), 7.30–7.44 (m, 4H, Ar-H), 7.57–7.68 (m, 3H, Ar-H), 7.74 (d,  $J = 8.0$  Hz, 1H, Ar-H), 8.41 (s, 1H, triazole), and 10.64 (s, 1H, NH);  $^{13}\text{C}$  NMR (100 MHz, DMSO- $d_6$ ,  $\delta$  ppm): 52.8, 63.2, 91.8, 115.6, 117.0, 121.3, 123.3, 124.7, 127.5, 127.9, 129.3, 133.3, 137.8, 141.3, 153.3, 162.0, and 164.8; HRMS calculated for  $\text{C}_{20}\text{H}_{14}\text{ClN}_4\text{O}_4$   $[\text{M}-\text{H}]^+$ : 409.0709 and found: 409.0715.

## 4.2 | Biological activity assays

### 4.2.1 | Antifungal activity

The antifungal activity was determined by the standard agar dilution method as per the CLSI (formerly NCCLS) guidelines.<sup>[56]</sup> The newly synthesized compounds were screened against five human pathogenic fungal strains, including *C. albicans* (NCIM 3471), *F. oxysporum* (NCIM 1332), *A. flavus* (NCIM 539), *A. niger* (NCIM 1196), and *C. neoformans* (NCIM 576). The standard miconazole and synthesized compounds were dissolved in DMSO. In phosphate buffer of pH 7, the medium yeast nitrogen base was dissolved and autoclaved for a duration of 10 min at 110°C. With each set, a growth control without the antifungal agent and solvent control DMSO were included. The fungal strains were freshly subcultured on Sabouraud dextrose agar and incubated at 25°C for 72 hr. The fungal cells were suspended in sterile distilled water and diluted to get 10<sup>5</sup> cells/ml. Then, 10 ml of the standardized suspension was inoculated on the control plates and the media were incorporated with the antifungal agents. The inoculated plates were incubated at 25°C for 48 hr. The readings were taken at the end of 48 and 72 hr. MIC is the lowest concentration of the drug preventing the growth of macroscopically visible colonies on the drug-containing plates when there is visible growth on the drug-free control plates.

### 4.2.2 | Antioxidant activity

Synthesized triazole-coumarin conjugates were screened for in vitro radical scavenging potential by using the DPPH radical scavenging assay. The results were compared with the standard synthetic antioxidant BHT.

The antioxidant activity of the synthesized compounds was assessed in vitro by the DPPH radical scavenging assay.<sup>[58]</sup> Results were compared with the standard antioxidant BHT. The hydrogen atom or electron-donating ability of the compounds was measured from the bleaching of the purple-colored methanol solution of DPPH. The spectrophotometric assay uses the stable radical DPPH as a reagent. Furthermore, 1 ml of various concentrations of the test compounds (5, 10, 25, 50, and 100 mg/ml) in methanol was added to 4 ml of 0.004% (w/v) methanol solution of DPPH. After a 30-min incubation period at room temperature, the absorbance was measured against blank at 517 nm. The percent inhibition (%) of free radical production from DPPH was calculated by the following equation:

$$\% \text{ scavenging} = [(A_{\text{control}} - A_{\text{sample}})/A_{\text{blank}}] \times 100,$$

where  $A_{\text{control}}$  is the absorbance of the control reaction (containing all reagents except the test compound) and  $A_{\text{sample}}$  is the absorbance of the test compound. Tests were carried out in triplicate.

## 4.3 | Molecular modeling study

### 4.3.1 | Homology modeling

The homology modeling technique was employed to build a 3D model structure of cytochrome P450 lanosterol 14 $\alpha$ -demethylase of *C. albicans* with the help of VLifeMDS 4.3 Promodel molecular modeling tool. The protein sequence was retrieved from UniprotKB database (accession number: P10613). The homologs' template sequence search was carried out against the protein structure database (<http://www.rcsb.org/>) by using BlastP. The appropriate template crystal structure of human lanosterol 14 $\alpha$ -demethylase (CYP51) complexes with miconazole (3LD6 B) which was based on default parameters, identity and positive criteria. The secondary structure assignment and sequence realignment were carried out to build the final modeled structure of fungal CYP51.

### 4.3.2 | Molecular docking study

The model protein structure and 3D structure of sketched synthesized compound were prepared for molecular docking using AutoDock Vina docking tool. The molecular docking study of synthesized compounds **7a-g** and **8a-g** was carried out using the final modeled structure of fungal CYP51. To understand this mechanism of action of inhibitors, molecular interactions were analyzed.

### 4.3.3 | ADMET testing

The ADMET properties of synthesized compounds **7a-g** and **8a-g** and standard drug were tested using FAFDrug2 tool, which is run on the Linux operating system.<sup>[59]</sup> The FAFDrug2 tool works on assumptions of Lipinski's rule of five and Veber's rule, which was widely followed in filtering lead compounds that would likely be further developed in drug design programs.<sup>[60]</sup> In addition to this, some other parameters were also considered to test ADMET properties, such as the number of rotatable bonds (>10), the number of rigid bonds, and percentage absorption (%ABS), which significantly contribute to good oral bioavailability and good intestinal absorption.<sup>[61]</sup>

## ACKNOWLEDGMENTS

S. V. A. is very grateful to the Council of Scientific and Industrial Research (CSIR), New Delhi, for providing a research fellowship. The authors are also grateful for providing laboratory facilities to the Head, Department of Chemistry, Dr. Babasaheb Ambedkar Marathwada University, Aurangabad.

## CONFLICTS OF INTERESTS

The authors declare that there are no conflicts of interests.

**ORCID**

 Satish V. Akolkar  <http://orcid.org/0000-0002-5467-4962>

 Jaiprakash N. Sangshetti  <http://orcid.org/0000-0002-9064-4111>

 Bapurao B. Shingate  <http://orcid.org/0000-0001-7207-0794>
**REFERENCES**

- [1] D. A. Enoch, H. A. Ludlam, N. M. Brown, *J. Med. Microbiol.* **2006**, 55, 809.
- [2] D. J. Sheehan, C. A. Hitchcock, C. M. Sibley, *Clin. Microbiol. Rev.* **1999**, 12, 40.
- [3] N. H. Georgopapadakou, T. J. Walsh, *Antimicrob. Agents Chemother.* **1996**, 40, 279.
- [4] M. A. Pfaller, *Am. J. Med.* **2012**, 125, S3.
- [5] A. Bistrovic, N. Stipanicev, T. Opacak-Bernardi, M. Jukic, S. Martinez, L. Glavas-Obrovac, S. Raic-Malic, *New J. Chem.* **2017**, 41, 7531.
- [6] Z. C. Dai, Y. F. Chen, M. Zhang, S. K. Li, T. T. Yang, L. Shen, J. X. Wang, S. S. Qian, H. L. Zhu, Y. H. Ye, *Org. Biomol. Chem.* **2015**, 13, 477.
- [7] N. Fu, S. Wang, Y. Zhang, C. Zhang, D. Yang, L. Weng, B. Zhao, L. Wang, *Eur. J. Med. Chem.* **2017**, 136, 596.
- [8] S. Zhang, Z. Xu, C. Gao, Q.-C. Ren, L. Chang, Z.-S. Lv, L.-S. Feng, *Eur. J. Med. Chem.* **2017**, 138, 501.
- [9] H. M. Faidallah, A. S. Girgis, A. D. Tiwari, H. H. Honkanadavar, S. J. Thomas, A. Samir, A. Kalmouch, K. A. Alamry, K. A. Khan, T. S. Ibrahim, A. Al-Mahmoudy, A. M. Asiri, S. S. Panda, *Eur. J. Med. Chem.* **2018**, 143, 1524.
- [10] Z. Xu, S.-J. Zhao, Y. Liu, *Eur. J. Med. Chem.* **2019**, 183, 111700.
- [11] Y. Tian, Z. Liu, J. Liu, B. Huang, D. Kang, H. Zhang, E. De Clercq, D. Daelemans, C. Pannecouque, K.-H. Lee, C. H. Chen, P. Zhan, X. Liu, *Eur. J. Med. Chem.* **2018**, 151, 339.
- [12] P. Yadav, J. K. Yadav, A. Agarwal, S. K. Awasthi, *RSC Adv.* **2019**, 9, 31969.
- [13] D. Dheer, V. Singh, R. Shankar, *Bioorg. Chem.* **2017**, 71, 30.
- [14] V. V. Rostovtsev, L. G. Green, V. V. Fokin, K. B. Sharpless, *Angew. Chem., Int. Ed.* **2002**, 41, 2596.
- [15] H. C. Kolb, K. B. Sharpless, *Drug Discov. Today* **2003**, 8, 1128.
- [16] G. C. Tron, T. Pirali, R. A. Billington, P. L. Canonico, G. Sorba, A. A. Genazzani, *Med. Res. Rev.* **2008**, 28, 278.
- [17] S. G. Agalave, S. R. Maujan, V. S. Pore, *Chem.-Asian J.* **2011**, 6, 2696.
- [18] N. M. Meghani, H. H. Amin, B.-J. Lee, *Drug Discov. Today* **2017**, 22, 1604.
- [19] K. Bozorov, J. Zhao, H. A. Aisa, *Bioorg. Med. Chem.* **2019**, 27, 3511.
- [20] N. S. Vatmurge, B. G. Hazra, V. S. Pore, F. Shirazi, P. S. Chavan, M. V. Deshpande, *Bioorg. Med. Chem. Lett.* **2008**, 18, 2043.
- [21] Y. C. Duan, Y. C. Ma, E. Zhang, X. J. Shi, M. M. Wang, X. W. Ye, H. M. Liu, *Eur. J. Med. Chem.* **2013**, 62, 11.
- [22] J. Zhang, H. Zhang, W. Cai, L. Yu, X. Zhen, A. Zhang, *Bioorg. Med. Chem.* **2009**, 17, 4873.
- [23] D. Huber, H. Hubner, P. Gmeiner, *J. Med. Chem.* **2009**, 52, 6860.
- [24] T. V. Soumya, C. M. Ajmal, D. Bahulayan, *Bioorg. Med. Chem. Lett.* **2017**, 27, 450.
- [25] J. Xiao, L. B. Lin, J. Y. Hu, D. Z. Duan, W. Shi, Q. Zhang, W. B. Han, L. Wang, X. L. Wang, *Tetrahedron Lett.* **2018**, 59, 1772.
- [26] Z. Xu, X. Wu, G. Li, Z. Feng, J. Xu, *Nat. Prod. Res.* **2019**, 34, 1002.
- [27] M. Zhao, L. Y. Yuan, D. Y. Guo, *Phytochemistry* **2018**, 148, 97.
- [28] R. Cai, Y. Wu, S. Chen, H. Cui, Z. Liu, C. Li, Z. She, *J. Nat. Prod.* **2018**, 81, 1376.
- [29] N. Rustamova, K. Bozorov, T. Efferth, A. Yili, *Phytochem. Rev.* **2020**, 19, 425.
- [30] H. Singh, J. V. Singh, K. Bhagat, H. K. Gulati, M. Sanduja, N. Kumar, N. Kinarivala, S. Sharma, *Bioorg. Med. Chem.* **2019**, 27, 3477.
- [31] P. O. Patil, S. B. Bari, S. D. Firke, P. K. Deshmukh, S. T. Donda, D. A. Patil, *Bioorg. Med. Chem.* **2013**, 21, 2434.
- [32] Y. Shi, C. Zhou, *Bioorg. Med. Chem. Lett.* **2011**, 21, 956.
- [33] P. M. Ronad, M. N. Noolvi, S. Sapkal, S. Dharbhamulla, V. S. Maddi, *Eur. J. Med. Chem.* **2010**, 45, 85.
- [34] R. Aggarwal, S. Kumar, P. Kaushik, D. Kaushik, G. K. Gupta, *Eur. J. Med. Chem.* **2013**, 62, 508.
- [35] T. Gregoric, M. Sedic, P. Grbcic, A. Tomljenovic Paravic, S. Kraljevic Pavelic, M. Cetina, R. Vianello, S. Raic-Malic, *Eur. J. Med. Chem.* **2017**, 125, 1247.
- [36] Y. C. Zheng, Y. C. Duan, J. L. Ma, R. M. Xu, X. Zi, W. L. Lv, M. M. Wang, X. W. Ye, S. Zhu, D. Mobley, Y. Y. Zhu, J. W. Wang, J. F. Li, Z. R. Wang, W. Zhao, H. M. Liu, *J. Med. Chem.* **2013**, 56, 8543.
- [37] J. Dandriyal, R. Singla, M. Kumar, V. Jaitak, *Eur. J. Med. Chem.* **2016**, 119, 141.
- [38] S. Z. Ferreira, H. C. Carneiro, H. A. Lara, R. B. Alves, J. M. Resende, H. M. Oliveira, L. M. Silva, D. A. Santos, R. P. Freitas, *ACS Med. Chem. Lett.* **2015**, 6, 271.
- [39] Y.-L. Fan, X. Ke, M. Liu, *J. Heterocycl. Chem.* **2018**, 55, 791.
- [40] M. H. Shaikh, D. D. Subhedar, F. A. K. Khan, J. N. Sangshetti, B. B. Shingate, *Chin. Chem. Lett.* **2016**, 27, 295.
- [41] K. Kushwaha, N. Kaushik, Lata, S. C. Jain, *Bioorg. Med. Chem. Lett.* **2014**, 24, 1795.
- [42] M. H. Shaikh, D. D. Subhedar, L. Nawale, D. Sarkar, F. A. K. Khan, J. N. Sangshetti, B. B. Shingate, *Mini-Rev. Med. Chem.* **2019**, 19, 1178.
- [43] S. P. Khare, T. R. Deshmukh, J. N. Sangshetti, V. S. Krishna, D. Sriram, V. M. Khedkar, B. B. Shingate, *ChemistrySelect* **2018**, 3, 13113.
- [44] M. H. Shaikh, D. D. Subhedar, B. B. Shingate, F. A. Kalam Khan, J. N. Sangshetti, V. M. Khedkar, L. Nawale, D. Sarkar, G. R. Navale, S. S. Shinde, *Med. Chem. Res.* **2016**, 25, 790.
- [45] S. V. Akolkar, A. A. Nagargoje, V. S. Krishna, D. Sriram, J. N. Sangshetti, M. Damale, B. B. Shingate, *RSC Adv.* **2019**, 9, 22080.
- [46] A. A. Nagargoje, S. V. Akolkar, M. M. Siddiqui, A. V. Bagade, K. M. Kodam, J. N. Sangshetti, M. G. Damale, B. B. Shingate, *J. Chin. Chem. Soc.* **2019**, 66, 1658.
- [47] D. D. Subhedar, M. H. Shaikh, B. B. Shingate, L. Nawale, D. Sarkar, V. M. Khedkar, F. A. Kalam Khan, J. N. Sangshetti, *Eur. J. Med. Chem.* **2017**, 125, 385.
- [48] M. H. Shaikh, D. D. Subhedar, M. Arkile, V. M. Khedkar, N. Jadhav, D. Sarkar, B. B. Shingate, *Bioorg. Med. Chem. Lett.* **2016**, 26, 561.
- [49] A. B. Danne, A. S. Choudhari, S. Chakraborty, D. Sarkar, V. M. Khedkar, B. B. Shingate, *MedChemComm* **2018**, 9, 1114.
- [50] M. H. Shaikh, D. D. Subhedar, L. Nawale, D. Sarkar, F. A. Kalam Khan, J. N. Sangshetti, B. B. Shingate, *MedChemComm* **2015**, 6, 1104.
- [51] T. R. Deshmukh, A. P. Sarkate, D. K. Lokwani, S. V. Tiwari, R. Azad, B. B. Shingate, *Bioorg. Med. Chem. Lett.* **2019**, 29, 126618.
- [52] G. Wang, Z. Peng, J. Wang, X. Li, J. Li, *Eur. J. Med. Chem.* **2017**, 125, 423.
- [53] P. Neeraja, S. Srinivas, K. Mukkanti, P. K. Dubey, S. Pal, *Bioorg. Med. Chem. Lett.* **2016**, 26, 5212.
- [54] G. Wang, Z. Peng, J. Wang, J. Li, X. Li, *Bioorg. Med. Chem. Lett.* **2016**, 26, 5719.
- [55] C. Ferroni, A. Pepe, Y. S. Kim, S. Lee, A. Guerrini, M. D. Parenti, A. Tesei, A. Zamagni, M. Cortesi, N. Zaffaroni, M. De Cesare, G. L. Beretta, J. B. Trepel, S. V. Malhotra, G. Varchi, *J. Med. Chem.* **2017**, 60, 3082.
- [56] Z. K. Khan, Proc. Int. Work. UNIDO-CDRI, 1997, pp. 210–211.
- [57] S. Zhang, Y. Luo, L.-Q. He, Z.-J. Liu, A.-Q. Jiang, Y.-H. Yang, H.-L. Zhu, *Bioorg. Med. Chem.* **2013**, 21, 3723.
- [58] M. Burits, F. Bucar, *Phyther. Res.* **2000**, 14, 323.
- [59] D. Lagorce, O. Sperandio, H. Galons, M. A. Miteva, B. O. Villoutreix, *BMC Bioinf.* **2008**, 9, 396.

- [60] C. A. Lipinski, F. Lombardo, B. W. Dominy, P. J. Feeney, *Adv. Drug Deliv. Rev.* **2001**, *46*, 3.
- [61] P. Ertl, B. Rohde, P. Selzer, *J. Med. Chem.* **2000**, *43*, 3714.

### SUPPORTING INFORMATION

Additional supporting information may be found online in the Supporting Information section.

**How to cite this article:** Akolkar SV, Nagargoje AA, Shaikh MH, et al. New *N*-phenylacetamide-linked 1,2,3-triazole-tethered coumarin conjugates: Synthesis, bioevaluation, and molecular docking study. *Arch Pharm.* 2020;353:e2000164. <https://doi.org/10.1002/ardp.202000164>